LETTER

doi:10.1038/nature12077

Corticostriatal neurons in auditory cortex drive decisions during auditory discrimination

Petr Znamenskiy[1,2] & Anthony M. Zador[2]

The neural pathways by which information about the acoustic world reaches the auditory cortex are well characterized, but how auditory representations are transformed into motor commands is not known. Here we use a perceptual decision-making task in rats to study this transformation. We demonstrate the role of corticostriatal projection neurons in auditory decisions by manipulating the activity of these neurons in rats performing an auditory frequency-discrimination task. Targeted channelrhodopsin-2 (ChR2)[1,2]-mediated stimulation of corticostriatal neurons during the task biased decisions in the direction predicted by the frequency tuning of the stimulated neurons, whereas archaerhodopsin-3 (Arch)[3]-mediated inactivation biased decisions in the opposite direction. Striatal projections are widespread in cortex and may provide a general mechanism for the control of motor decisions by sensory cortex.

After reaching the cortex, auditory information is processed and relayed to a number of cortical and subcortical targets by distinct, largely non-overlapping populations of pyramidal neurons. These targets include parietal cortex, secondary auditory areas, inferior colliculus and striatum, regions that have distinct roles in perception and behaviour. How these outputs help to establish associations between sounds and motor responses is unknown.

We sought to test the hypothesis that the projection from the auditory cortex to the striatum carries acoustic information that drives behavioural choices during auditory discrimination. The striatum receives topographic inputs from throughout the cortex. Striatal regions that receive input from motor and prefrontal cortices have been implicated in a wide range of cognitive processes, including decision-making[4], action selection[5] and reinforcement learning[6,7]. Through downstream structures of the basal ganglia, the striatum influences the activity in the motor thalamus[8] as well as superior colliculus[9], a structure that has been implicated in driving behavioural choices in two-alternative choice tasks[10]. Plasticity of corticostriatal connections may enable them to encode the arbitrary stimulus–response associations that are acquired in such tasks[11].

In contrast, the function of striatal regions that receive direct input from sensory cortical areas is less well established. The striatum is one of the major long-range targets of the auditory cortex[12]. The auditory cortex projects to a specific region of the striatum[13]. This striatal region does not receive input from any other cortical area and contains neurons sensitive to auditory stimuli[14,15]. We set out to test whether the auditory corticostriatal projection drives choices during auditory discrimination.

We first developed a novel auditory discrimination task, inspired by experiments in primate middle temporal area (area MT)[16], that was designed to exploit the tonotopic organization of the auditory system[17]. We trained rats to discriminate low- and high-frequency 'cloud-of-tones' stimuli in a two-alternative choice task[18] (Fig. 1a). On each trial the stimulus consisted of a train of short overlapping pure tones distributed over a three-octave range (5–40 kHz). Subjects were required to choose between a left and a right reward port depending on whether the stimulus contained mostly low-frequency (5–10 kHz) or high-frequency (20–40 kHz) tones (Fig. 1b). Rats were free to withdraw and report their choice at any time after the onset of the stimulus. Rats readily learned this task. Performance varied smoothly with stimulus difficulty, and approached 100% on the easiest stimuli (Fig. 1c).

We used tetrode recordings to characterize the activity of individual neurons in the auditory cortex and the auditory striatum while rats performed the task. Auditory striatal neurons have been characterized previously in anaesthetized and passively listening animals[14,15] but not during behaviour. The firing rates of neurons in both auditory cortex and striatum varied monotonically with the stimulus (Supplementary Fig. 1a, b, e, f). 'Ideal observer' analysis showed that stimulus selectivity of cortical and striatal neurons was similar (Supplementary Fig. 1c, d, g, h). Although individual neurons rarely matched the performance of the rats, many neurons in both areas could discriminate the stimulus above chance levels (Supplementary Fig. 1d, h). These observations indicate that neurons in the striatum preserve the information available to perform the cloud-of-tones task.

We then tested whether manipulating cortical activity with ChR2 (refs 1, 2) could affect subjects' choices in the task. We proposed that activation of auditory cortical neurons in different regions of the tonotopic map would result in choice biases, the directions of which would depend on the frequency–response association that the rat had been trained to make. We implanted arrays of optical fibres coupled to tetrodes (Supplementary Fig. 2), which enabled us to characterize the frequency preference of neurons near the fibre tip. We activated ChR2-expressing auditory cortex neurons on a subset of trials, and

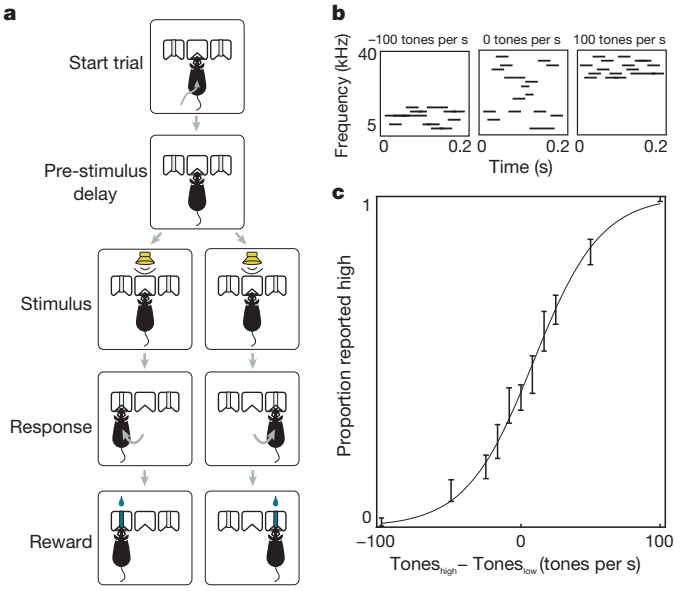

Figure 1 | Cloud-of-tones task. **a**, Format of the behavioural task. **b**, Example stimulus spectrograms at −100, 0 and +100 tones per s. **c**, Psychometric curve from a single rat (error bars, 95% confidence interval).

[1]Watson School of Biological Sciences, Cold Spring Harbor Laboratory, 1 Bungtown Road, Cold Spring Harbor, New York 11724, USA. [2]Cold Spring Harbor Laboratory, 1 Bungtown Road, Cold Spring Harbor, New York 11724, USA.

compared performance on stimulated trials to that on control trials without light activation. To minimize behavioural adaptation to photostimulation, we limited the number of stimulation trials to 25% of the total trials, and rewarded the animal as in control trials, according to the frequency content of the stimulus. To quantify the effects of photostimulation on subjects' behaviour, we fit a logistic regression model to the subjects' choices (see Methods), estimating what change to the auditory stimulus would produce a behavioural effect equivalent to that of photostimulation.

We first expressed ChR2 non-specifically in the primary auditory cortex using adeno-associated virus (AAV). ChR2 expression was distributed throughout layers II to V and was present, although to a lesser extent, in layer VI (Supplementary Fig. 3a, b). In some sessions, activation of ChR2-expressing neurons induced substantial biases (Supplementary Fig. 3c). However, contrary to our expectations the direction of the bias was not predicted by the tuning of the neurons near the fibre (Supplementary Fig. 3f). Moreover, this non-specific activation not only biased subjects' choices but also interfered with their ability to perform the task, as measured by the slope of the psychometric curve (Supplementary Fig. 3d, e).

The lack of correspondence between the direction of stimulation-evoked choice biases and frequency tuning was surprising and has several possible explanations. First, these choice biases may result from activation of intracortical projection neurons from other frequency bands of the auditory cortex. Second, they may arise from preferential activation of local interneurons in response to synchronous activation of a large number of cortical cells. Third, these biases may be a consequence of stimulation of competing output pathways, projecting to target areas with different functional roles. Consistent with this third possibility, stimulation resulted in predominantly contralateral biases (36 out of 57 sites, $P = 0.015$, Supplementary Fig. 3g, h), suggesting the activation of a lateralized motor pathway. These results suggested that the auditory cortex plays a role in the task, but that the method of non-specific activation of diverse neuronal populations used in these experiments does not provide sufficient experimental control over the activity of the projection neurons driving choices in this behaviour. We therefore proposed that targeted stimulation of corticostriatal neurons might produce more systematic effects.

We used two complementary strategies to test the role of the neuronal subpopulation in auditory cortex that projects to the striatum. In the first strategy, we targeted ChR2 specifically to corticostriatal neurons using a herpes simplex virus-1 (HSV-1) engineered to express Cre recombinase[19–21] (Fig. 2a). This virus, when injected into the auditory striatum, was transported retrogradely along the axons and drove Cre expression in corticostriatal neurons. We then injected a Cre-dependent AAV driving expression of ChR2 into the auditory cortex, resulting in expression of ChR2 only in neurons infected by both the HSV-1–Cre and the AAV-ChR2. Most (84%) of ChR2-expressing neurons were located in layer V (Fig. 2c, d), consistent with previous results[22].

Pulses of blue light delivered through fibres in the cortex reliably drove action potentials in a small population of presumed corticostriatal neurons (Fig. 2b; only 4 of 201 cells responded in more than 50% of trials). Across sites, stimulation consistently biased subjects' choices towards the choice port associated with the preferred frequency of the stimulation site (Fig. 2e, f). The biases were not significant in individual sessions ($P < 0.05$ in only 1 out of 33 sessions), partly because the number of stimulated trials per session was typically small (70 ± 24 ($\pm$ s.d.) trials). In contrast to non-specific stimulation, contralateral and ipsilateral biases were observed with similar frequency (12 out of 33 contralateral sites, $P = 0.31$, signed-rank test) and subjects' psychophysical performance was not impaired (Supplementary Fig. 4a). Choice biases were not observed in uninjected controls (Fig. 2g and Supplementary Fig. 5a), indicating that they were driven by the ChR2-mediated activation of corticostriatal neurons and not non-specific effects of light delivery. Thus, activation of corticostriatal neurons biased behaviour in a manner predicted by their frequency tuning.

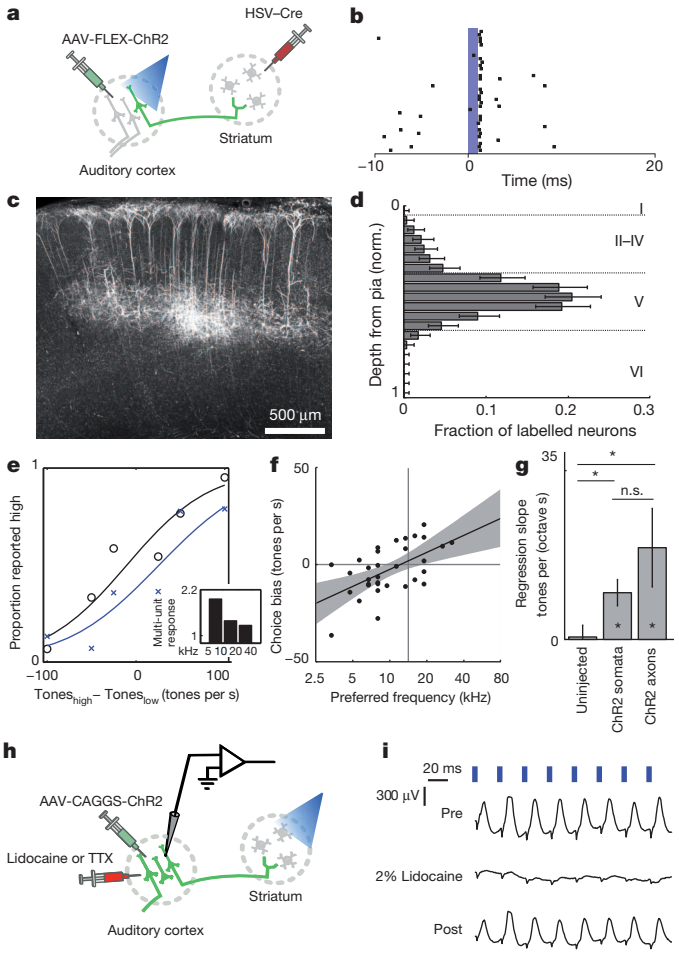

Figure 2 | ChR2 stimulation of corticostriatal neurons biases subjects' choices. **a**, Strategy targeting ChR2 expression to corticostriatal neurons using retrograde HSV–Cre and AAV-FLEX-ChR2, where ChR2 expression is controlled by the Cre-dependent FLEX switch. **b**, A corticostriatal neuron identified on the basis of its short latency light-evoked response (approximately 1 ms). Blue bar indicates the timing of the light pulse (10 mW, 1 ms duration). **c**, ChR2 expression in corticostriatal neurons. **d**, Depth distribution of ChR2 expression. Dashed lines mark the approximate location of layer boundaries. Error bars, 95% confidence intervals. **e**, Psychometric performance during a behavioural session in control trials (black) and during stimulation of corticostriatal neurons (blue). $P = 0.02$ for stimulation-evoked choice bias. Inset shows frequency tuning of multi-unit responses normalized to baseline, binned by octave. **f**, Across the population, the direction and magnitude of choice biases evoked by stimulation depend on the frequency preference of the stimulation site ($n = 33$ sites from 2 rats, $P = 0.0006$ for linear regression of choice bias and frequency preference). Grey shading, 95% confidence interval for regression line. **g**, Dependence of choice bias on preferred frequency of the stimulation site in uninjected controls, and during specific stimulation of corticostriatal neurons and their axons. $^*P < 0.05$; n.s., not significant, error bars are standard error through bootstrap. P values within bars compare the frequency dependence of choice bias to 0. **h**, Strategy for the inactivation of recurrent cortical activity during stimulation of striatal axons. TTX, tetrodotoxin. CAGGS, chicken β-actin promoter and cytomegalovirus early enhancer. **i**, Lidocaine infusion into the auditory cortex reversibly abolishes antidromic light-evoked local field potential responses.

The behavioural effects of photostimulation could arise either directly through excitation of striatal neurons by their cortical inputs, or indirectly through excitation of other output pathways of the auditory cortex through recurrent connections. Excitation of corticostriatal neurons resulted in general suppression of local cortical activity (Supplementary Fig. 6), favouring the hypothesis that behavioural effects of photostimulation are mediated by long-range rather than local outputs of these neurons.

To test this hypothesis directly, we used a second strategy. This strategy did not rely on cortical stimulation and therefore enabled us to test whether stimulation of corticostriatal neurons could bias subjects' choices when recurrent cortical activity was blocked. We stimulated the axons of corticostriatal neurons in the striatum while inhibiting the recurrent cortical excitation pharmacologically (Fig. 2h). To define the frequency tuning of stimulated fibres, we exploited the topography of corticostriatal projections[23]. We confirmed the topographic organization of the striatal projection of the auditory cortex in rats through retrograde (Supplementary Fig. 7) tracing. Owing to this topography, focal light stimulation in the striatum excites corticostriatal axons arising from a restricted region of the tonotopic map. We used striatal multi-unit activity to characterize the frequency preference of the striatal stimulation site.

Stimulation of corticostriatal axons biased subjects' choices towards the choice port associated with the preferred frequency of the stimulation site (Fig. 2g and Supplementary Fig. 5b). Stimulation also had a modest effect on the subjects' performance at sites with large choice biases, possibly owing to a ceiling effect (Supplementary Fig. 4b, c). Thus, both direct activation of corticostriatal somata in the cortex, as well as antidromic activation of corticostriatal terminals in the striatum, biased the rats' choices in a manner predicted from the frequency tuning of the activated neurons.

We next tested whether stimulation of the axons of corticostriatal neurons could bias subjects' choices in the absence of cortical recurrent activity. We selected striatal sites whose stimulation produced significant biases ($P < 0.05$) in subjects' choices and repeated stimulation after pharmacologically inactivating the ipsilateral auditory cortex. Cortical inactivation (2% lidocaine, $n = 2$ sites; 125 μM tetrodotoxin, $n = 5$ sites) blocked antidromic light-evoked local field potentials (Fig. 2i). Photostimulation of corticostriatal axons still biased choices in the absence of cortical activity ($P = 0.016$, signed-rank test, Supplementary Figs 8 and 9), demonstrating that these biases are mediated directly by long-range outputs of corticostriatal neurons.

We next examined the effects of stimulation of corticostriatal neurons on rats' response times. Although individual rats varied in how they prioritized response speed versus response accuracy (Supplementary Fig. 10a–f), most rats used in the stimulation and inactivation experiments showed a small but significant increase (in the order of 20 to 50 ms) in response time on challenging trials, consistent with that reported previously in rats[18]. We quantified the shift of the chronometric curve produced by stimulation of corticostriatal neurons (Supplementary Fig. 10g, h). Across sessions, stimulation shifted chronometric curves, mimicking the effect of adding acoustic evidence favouring the choice associated with the preferred frequency of the stimulation site (Supplementary Fig. 10i, j).

So far, our results establish that activation of the corticostriatal pathway is sufficient to bias subjects' choices during an auditory discrimination task, but do not establish whether corticostriatal activity contributes to the formation of decisions under normal conditions, in the absence of ChR2 activation. If corticostriatal spikes are important under normal conditions, then suppressing these spikes during the task should lead to an 'anti-bias'; that is, a bias in the direction opposite to that induced by ChR2 activation. To test this hypothesis, we targeted the expression of the light-activated proton pump Arch[3] to corticostriatal neurons using the HSV-1-based approach described above (Fig. 3a). Rather than attempting to inactivate all corticostriatal cells—a technically difficult feat whose interpretation may be obscured by the compensatory plasticity common to lesion studies—we sought instead to silence corticostriatal neurons within a restricted region of the tonotopic map.

Pulses of green light in Arch-expressing animals inhibited spiking of putative corticostriatal neurons (Fig. 3b). As predicted, inactivation of corticostriatal neurons biased subjects' choices away from the reward port associated with the frequency band of the inactivation site (Fig. 3c) but did not affect subjects' sensitivity quantified as the slope of the

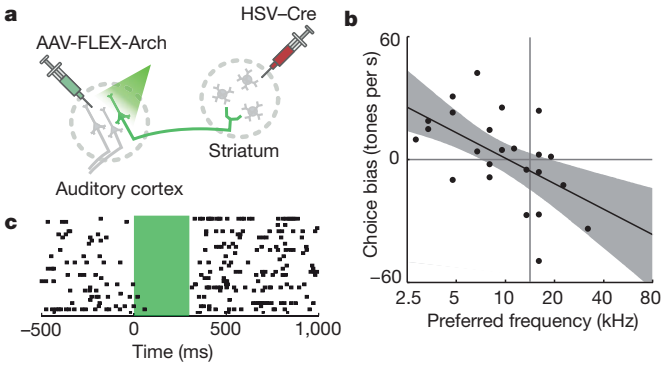

Figure 3 | Arch-mediated inactivation of corticostriatal neurons anti-biases subjects' choices. **a**, Strategy targeting Arch expression to corticostriatal neurons. **b**, Activity of a presumed corticostriatal neuron inhibited by pulses of green light. Green shading shows the timing of the light pulse (300 ms, 5 mW). **c**, Inactivation biased choices away from the direction associated with the preferred frequency of the inactivation site ($n = 24$ sites from 3 rats, $P = 0.0043$ for linear regression of choice bias and frequency preference). Grey shading, 95% confidence interval for regression line.

psychometric curve (Supplementary Fig. 4d). A similar trend was reflected in the subjects' chronometric functions but did not reach significance (Supplementary Fig. 11k, l). Pulses of green light did not affect the behaviour of uninjected control animals (Supplementary Fig. 5c). These results indicate that corticostriatal neurons in the auditory cortex transmit signals used by rats to make decisions driven by sounds.

These experiments provided us with an opportunity to quantify the contribution of the output of single corticostriatal cells to behaviour. Earlier studies showed that subjects can be trained to detect the artificial stimulation of as few as 6 to 197 neurons[24] or even a single neuron[25]. Our experiments allow us to estimate the contribution of single neurons to behaviour during normal perception.

We tagged Arch with green fluorescent protein (Arch–GFP) to estimate the number of neurons silenced in each experiment (Fig. 4b). Using *in vivo* recordings of putative corticostriatal cells, we estimated that the efficiency of inactivation decayed with a space constant of approximately 564 μm (Fig. 4a and Supplementary Fig. 11). We quantified the number of Arch-expressing neurons within a radius of 1 mm, or approximately two space constants, from the inactivation fibre for each session. The magnitude of choice biases depended on the number of corticostriatal neurons expressing Arch near the fibre (Fig. 4c). Robust choice biases were observed for sites with 1,040 to 2,444 Arch-expressing neurons within 1 mm of the fibre, comprising 0.35 to 0.83% of neurons in that

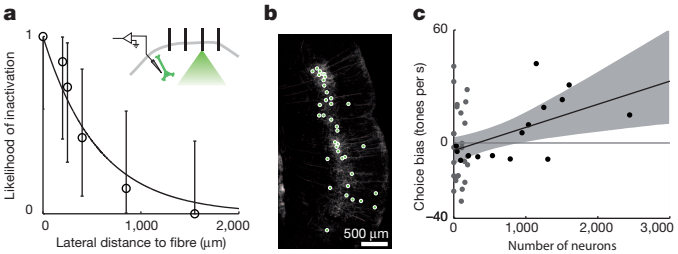

Figure 4 | Estimation of numbers of neurons affected by Arch inactivation. **a**, The likelihood of silencing for Arch-expressing corticostriatal neurons as a function of distance from the fibre ($n = 7$). Error bars, 95% binomial confidence intervals. **b**, Somata of neurons expressing Arch-GFP (green circles) identified in a fluorescence image of the auditory cortex at the end of an inactivation experiment. **c**, Effects of inactivation at sites tuned <10 kHz or >20 kHz were correlated with the number of Arch-expressing neurons near the fibre ($n = 41$ sites from 5 rats, $P = 0.021$ for linear regression of choice bias and neuron number). Grey points are data for 2 out of 5 rats, for which Arch expression was low throughout the auditory cortex (on average 72 ± 69 cells per site). Grey shading, 95% confidence interval for regression line.

volume. Our observation that inactivation of this minute fraction of cells targeted to corticostriatal neurons could affect behaviour suggests a privileged role of these cells in auditory discrimination.

The size of the neuronal pool accounting for behavioural performance in psychophysical tasks is much smaller than the number neurons which carry signals relevant to the task[26]. The redundancy arising from correlated neuronal firing may restrict the effective size of the pool[26], limiting psychophysical performance. Our results suggest that the finite bandwidth provided by a small number of projection neurons that drive decisions constitutes an additional constraint limiting the effective pool size and therefore psychophysical performance.

We have shown that the striatal projection of the auditory cortex conveys signals that drive behavioural choices during performance of an auditory discrimination task. Although our results do not exclude the participation of other parallel pathways, the ubiquity of corticostriatal projections in cortex may provide a general mechanism for control of motor decisions by sensory context[27].

METHODS SUMMARY

Male Long Evans rats (Taconic Farms) were trained in a two-alternative choice discrimination task. Animal procedures were approved by the Cold Spring Harbour Laboratory Animal Care and Use Committee and carried out in accordance with National Institutes of Health standards.

Full Methods and any associated references are available in the online version of the paper.

Received 16 November 2012; accepted 14 March 2013.
Published online 1 May 2013.

1. Nagel, G. *et al.* Channelrhodopsin-2, a directly light-gated cation-selective membrane channel. *Proc. Natl Acad. Sci. USA* **100,** 13940–13945 (2003).
2. Boyden, E. S., Zhang, F., Bamberg, E., Nagel, G. & Deisseroth, K. Millisecond-timescale, genetically targeted optical control of neural activity. *Nature Neurosci.* **8,** 1263–1268 (2005).
3. Chow, B. Y. *et al.* High-performance genetically targetable optical neural silencing by light-driven proton pumps. *Nature* **463,** 98–102 (2010).
4. Ding, L. & Gold, J. I. Caudate encodes multiple computations for perceptual decisions. *J. Neurosci.* **30,** 15747–15759 (2010).
5. Kimchi, E. Y. & Laubach, M. Dynamic encoding of action selection by the medial striatum. *J. Neurosci.* **29,** 3148–3159 (2009).
6. Reynolds, J. N., Hyland, B. I. & Wickens, J. R. A cellular mechanism of reward-related learning. *Nature* **413,** 67–70 (2001).
7. Pasupathy, A. & Miller, E. K. Different time courses of learning-related activity in the prefrontal cortex and striatum. *Nature* **433,** 873–876 (2005).
8. Beckstead, R. M., Domesick, V. B. & Nauta, W. J. Efferent connections of the substantia nigra and ventral tegmental area in the rat. *Brain Res.* **175,** 191–217 (1979).
9. Hopkins, D. A. & Niessen, L. W. Substantia nigra projections to the reticular formation, superior colliculus and central gray in the rat, cat and monkey. *Neurosci. Lett.* **2,** 253–259 (1976).
10. Felsen, G. & Mainen, Z. F. Neural substrates of sensory-guided locomotor decisions in the rat superior colliculus. *Neuron* **60,** 137–148 (2008).
11. Kreitzer, A. C. & Malenka, R. C. Striatal plasticity and basal ganglia circuit function. *Neuron* **60,** 543–554 (2008).
12. Allen Brain Institute. Allen Mouse Connectivity Atlas http:// connectivity.brain-map.org (2012).
13. McGeorge, A. J. & Faull, R. L. The organization of the projection from the cerebral cortex to the striatum in the rat. *Neuroscience* **29,** 503–537 (1989).
14. Bordi, F. & LeDoux, J. Sensory tuning beyond the sensory system: an initial analysis of auditory response properties of neurons in the lateral amygdaloid nucleus and overlying areas of the striatum. *J. Neurosci.* **12,** 2493–2503 (1992).
15. Bordi, F., LeDoux, J., Clugnet, M. C. & Pavlides, C. Single-unit activity in the lateral nucleus of the amygdala and overlying areas of the striatum in freely behaving rats: rates, discharge patterns, and responses to acoustic stimuli. *Behav. Neurosci.* **107,** 757–769 (1993).
16. Salzman, C. D., Britten, K. H. & Newsome, W. T. Cortical microstimulation influences perceptual judgements of motion direction. *Nature* **346,** 174–177 (1990).
17. Sally, S. L. & Kelly, J. B. Organization of auditory cortex in the albino rat: sound frequency. *J. Neurophysiol.* **59,** 1627–1638 (1988).
18. Uchida, N. & Mainen, Z. F. Speed and accuracy of olfactory discrimination in the rat. *Nature Neurosci.* **6,** 1224–1229 (2003).
19. Lilley, C. E. *et al.* Multiple immediate-early gene-deficient herpes simplex virus vectors allowing efficient gene delivery to neurons in culture and widespread gene delivery to the central nervous system *in vivo*. *J. Virol.* **75,** 4343–4356 (2001).
20. Lima, S. Q., Hromádka, T., Znamenskiy, P. & Zador, A. M. PINP: a new method of tagging neuronal populations for identification during *in vivo* electrophysiological recording. *PLoS ONE* **4,** e6099 (2009).
21. Ciocchi, S. *et al.* Encoding of conditioned fear in central amygdala inhibitory circuits. *Nature* **468,** 277–282 (2010).
22. Reiner, A., Jiao, Y., Del Mar, N., Laverghetta, A. V. & Lei, W. L. Differential morphology of pyramidal tract-type and intratelencephalically projecting-type corticostriatal neurons and their intrastriatal terminals in rats. *J. Comp. Neurol.* **457,** 420–440 (2003).
23. Reale, R. A. & Imig, T. J. Auditory cortical field projections to the basal ganglia of the cat. *Neuroscience* **8,** 67–86 (1983).
24. Huber, D. *et al.* Sparse optical microstimulation in barrel cortex drives learned behaviour in freely moving mice. *Nature* **451,** 61–64 (2008).
25. Houweling, A. R. & Brecht, M. Behavioural report of single neuron stimulation in somatosensory cortex. *Nature* **451,** 65–68 (2008).
26. Britten, K. H., Shadlen, M. N., Newsome, W. T. & Movshon, J. A. The analysis of visual motion: a comparison of neuronal and psychophysical performance. *J. Neurosci.* **12,** 4745–4765 (1992).
27. Jiang, H., Stein, B. E. & McHaffie, J. G. Physiological evidence for a trans-basal ganglia pathway linking extrastriate visual cortex and the superior colliculus. *J. Physiol. (Lond.)* **589,** 5785–5799 (2011).

Supplementary Information is available in the online version of the paper.

Acknowledgements We thank B. Burbach for technical assistance, A. Reid for generating the AAV-FLEX-Arch–GFP construct and members of the Kepecs laboratory (CSHL) for the tetrode and fibre drive design. We thank K. Britten for comments and suggestions on the manuscript. AAV-CAGGS-ChR2-Venus plasmid was provided by K. Svoboda. AAV-CAGGS-FLEX-ChR2-tdTomato virus was a gift from A. Kepecs. AAV-CAG-Arch–GFP plasmid was provided by E. Boyden. AAV-EF1a-FLEX-ChR2-YFP was provided by K. Deisseroth. HSV–iCre-2A-Venus and HSV–mCherry-IRES–iCre constructs were provided by A. Luthi and packaged by BioVex. This work was supported by grants from the Swartz Foundation and the National Institutes of Health (grant numbers 25041001 and 55120101).

Author Contributions P.Z. and A.M.Z. designed the experiments, P.Z. carried out the experiments, and P.Z. and A.M.Z. analysed the data and wrote the manuscript.

Author Information Reprints and permissions information is available at www.nature.com/reprints. The authors declare no competing financial interests. Readers are welcome to comment on the online version of the paper. Correspondence and requests for materials should be addressed to A.M.Z. (zador@cshl.edu).

METHODS

Viral production. AAV-CAGGS-ChR2-Venus plasmid was used for non-specific cortical stimulation. AAV-CAGGS-FLEX-ChR2-tdTomato virus was used for targeted stimulation of corticostriatal neurons. AAV-FLEX-Arch–GFP construct was generated by subcloning Arch–GFP from an AAV-CAG-Arch–GFP plasmid into AAV-FLEX backbone from AAV-EF1a-FLEX-ChR2–YFP. The plasmid DNA was prepared using standard Maxiprep protocols (Qiagen). AAV serotype 2/9 was packaged by the University of North Carolina viral core at a titre of 1 to 2×10^{12} particles per ml. HSV–mCherry-IRES–iCre construct (for targeting Arch expression) and HSV–iCre-2A-Venus construct (for targeting ChR2 expression) were packaged at titres of 2.4×10^{10} and 3×10^{9} transducing units per ml.

Animal subjects. Animal procedures were approved by the Cold Spring Harbour Laboratory Animal Care and Use Committee and carried out in accordance with National Institutes of Health standards. Male Long Evans rats (Taconic Farms) were housed with free access to food, but were water restricted after the start of behavioural training. Water was available during task performance (24 µl for each correct trial) and freely available for 15 to 30 min after the end of each behavioural sessions and for at least 1 h on days when behavioural sessions were not conducted.

Viral injection. Three- to five-week-old rats were anaesthetized with a mixture of ketamine (60 mg kg^{-1} of body weight) and medetomidine (0.24 mg kg^{-1}) and placed in a stereotaxic apparatus. To target the auditory cortex, part of the temporalis muscle was resected to expose the temporoparietal suture, which was used as a landmark to target injections. For optogenetic experiments, four injections were made unilaterally spanning primary auditory cortex at 0.5, 1.5, 2.5 and 3.5 mm from the rostral edge of parietal bone and 1.2 mm from its ventral edge. A small craniotomy was made for each injection and a glass micropipette was inserted perpendicular to the surface of the brain. Two injections were made at the depths of 400 and 800 µm, expelling approximately 250 nl of virus at each depth. To target the auditory striatum, two small craniotomies were made 2.0 and 2.5 mm caudal of Bregma and 4.5 mm lateral of the midline. Injections were made at depths between 3.5 and 6 mm, 0.5 mm between injection sites, approximately 100 nl per site. Injections were carried out by delivering brief pulses of pressure using Picospritzer II (Parker), each pulse delivering approximately 2 nl at 0.2 Hz. Rats were monitored during their recovery from surgery and returned to group housing.

Behavioural training. The cloud-of-tones stimulus consisted of stream of 30-ms overlapping pure tones presented at 100 Hz (that is, with 10 ms between tone onsets). Eighteen possible tone frequencies were logarithmically spaced between 5 and 40 kHz, a range in which rats' hearing thresholds are low and relatively constant[28]. For each trial either the low (5 to 10 kHz) or the high (20 to 40 kHz) octave was selected as the target octave. Stimulus strength r determined the difference in the rate of high and low octave tones in the stimulus. Tones were drawn from the target octave with a probability of $(1 + 2r/100)/3$. The stream of tones continued until the rat withdrew from the centre port.

After reaching a weight of 200 to 250 g, rats were placed on a water deprivation schedule and behavioural training commenced. The rats were placed in a soundproof behavioural chamber and presented with three choice ports. The rats were trained to first poke into the centre port, wait for the onset of the auditory stimulus and select one of the other two ports to receive a water reward (24 µl). Rats were trained to carry out this sequence using the following procedure. During the first phase of training, water was delivered at the correct choice port as soon as the stimulus was played. The duration of the pre-stimulus delay, during which the rat was required to remain in the centre port, was drawn from an exponential distribution whose mean was gradually increased from 0.05 s to 0.3 s. The next phase of training required the rat to poke at the correct choice port to trigger water delivery. However, the rat was allowed to correct his choice if it made a mistake. When rats had learned to perform the discrimination so that they consistently scored higher than expected by chance, they were required to make the correct choice on the first attempt. Error trials were punished with a 4-s timeout (2 s during recording sessions). Initially, rats were trained to discriminate tone-cloud stimuli composed of tones either entirely in the high octave or entirely in the low octave ($r = 100$) and were gradually introduced to increasingly difficult stimuli.

Sound intensity of individual tones was constant during each trial. To discourage subjects from using loudness differences in discrimination, tone intensity was randomly selected on each trial from a uniform distribution 45 to 75 dB (SPL) during training. During manipulation and recording sessions, sound intensity was kept constant at 60 dB.

Electrophysiology and optogenetics. Custom-built optical fibre and tetrode arrays were assembled in-house. Each array carried 6 multimodal optical fibres 62.5 µm in diameter with a 50-µm core. The fibre tips were sharpened to a point using a diamond wheel to improve tissue penetration and increase the angle of the light exit cone. Each fibre was glued to a tetrode and the tetrode tip was cut to terminate within approximately 100 µm of the fibre tip. The fibre and tetrode assemblies were mounted on individually movable microdrives. The tetrodes were gold-plated to an impedance of 300 kΩ at 1 kHz and the tetrode and fibre tips were coated with DiI fluorescent dye (Life Technologies) to assist with the identification of fibre tracks in brain tissue.

To implant the fibre and tetrode array, rats were anaesthetized with a mixture of ketamine (40 mg kg^{-1} of body weight) and medetomidine (0.16 mg kg^{-1}) and placed in a stereotaxic apparatus. A craniotomy was made over the target area (for auditory cortex, 3.5 to 6.0 mm caudal of Bregma and 6.5 to 7.0 mm lateral from the midline; for auditory striatum, 2.5 to 3.5 mm caudal of Bregma and 4 to 5 mm lateral from the midline). All rats, with the exception of one Arch-expressing and one uninjected control animal, were implanted in the left hemisphere. The dura was removed and the implant was placed over the target area and fixed in place with dental acrylic. The tetrodes were then lowered until the first action potentials were encountered.

To characterize the frequency tuning of stimulation and inactivation sites, the rats were placed in a soundproof chamber and pure tones were played in free field at approximately 0.5 Hz. Tone frequencies spanned from 1 to 64 kHz and were played in a random order at 30, 50 or 70 dB-SPL. Only sites that significantly responded to sounds ($P < 0.01$, signed-rank test comparing firing rate 5 to 55 ms after sound onset to 0 to 50 ms preceding sound onset) were included in the analysis of stimulation and inactivation experiments. To determine the preferred frequency, firing rates in the window from 5 to 55 ms after sound onset were computed for each frequency at 70 dB. The resulting tuning curve was smoothed with a half-octave sliding window. The peak of the smoothed tuning curve was selected as the preferred frequency. Sites tuned to frequencies more than one octave outside the range used in the task (below 2.5 kHz) were excluded from analysis.

For optogenetic manipulations, laser light was coupled into a FC/PC parch cord using a FibrePort Collimator (Thor Labs). Laser power was adjusted to produce the desired output at the end of the patch cord. A single implanted fibre was selected for manipulation and coupled to the patch cord. For ChR2 activation, 473-nm laser light (10 mW) was delivered in 1-ms pulses (except at nine sites corticostriatal stimulation sites, at which we used 0.5 ms pulses) at 40 Hz while the rat remained in the centre port. For Arch, 530-nm laser light (50 mW) was delivered in 1-ms pulses (except at six sites at which we used 0.5-ms pulses) at 100 Hz, which produced an average power of 5 mW. To decrease the ability of the rat to detect the stimulation light, a mask light-emitting diode (LED) of a wavelength similar to that of the laser was placed above the centre port in the behaviour chamber. The mask LED was activated on control as well as stimulation trials in the same temporal pattern as the laser. Manipulation trials were randomly interleaved among control trials. The optical fibre was advanced approximately 300 µm between manipulation sessions.

For action potential recordings, signals were filtered 600 to 6,000 Hz and recorded using the Neuralynx Cheetah 32 system and Cheetah data acquisition software.

Pharmacological inactivation. Two PEEK tubing cannulas (Plastics One) were implanted into the auditory cortex with a separation of approximately 1 mm. Six stereotrodes were implanted alongside the cannulas, spanning 3 to 4 mm of the auditory cortex, to confirm the efficiency of inactivation. One hour before the start of the behavioural session, the animal was briefly anaesthetized with 2% isofluorane and 0.4 µl of drug (during inactivation sessions) or 9 g l^{-1} NaCl (during control sessions) was injected at the rate of 0.08 µl min^{-1} in both cannulas.

Analysis of behaviour data. Although each trial had a target frequency distribution, which determined which choice port was to be rewarded, as rats sampled the stimulus for a finite period of time, the frequency distribution they experienced might have been substantially different from the target. Therefore, we determined the rate of presentation of high and low tones (f_{high} and f_{low}), that is, the number of tones divided by the reaction time, that the rats actually heard on each trial. To quantify rats' behaviour, psychometric curves were fit with a logistic regression model:

$$\ln \frac{p}{1-p} = \beta_0 + \beta_1 (f_{high} - f_{low}) \quad (1)$$

where p is the fraction of choices towards the port associated with high frequencies. Parameters β_0 and β_1 measure the bias and slope of the psychometric curve, respectively. To quantify the effects of stimulation or inactivation, we extended the model to incorporate the effects of these manipulations:

$$\ln \frac{p}{1-p} = \beta_0 + \beta_1 (f_{high} - f_{low}) + \beta_2 S + \beta_3 S (f_{high} - f_{low})$$

where S is 1 on manipulation trials and 0 on control trials. The choice bias evoked by the manipulation is $\beta_2 / (\beta_1 + \beta_3)$ tones per s. In experiments in which ChR2 or Arch expression was specifically targeted to corticostriatal neurons, the interaction term β_3 was not significantly different from 0 and was omitted in estimates of choice bias:

$$\ln\frac{p}{1-p}=\beta_0+\beta_1(f_{high}-f_{low})+\beta_2 S$$

The light-evoked choice bias is then β_2/β_1 tones per s. Confidence intervals and P values for individual manipulation sessions were estimated from standard errors of regression coefficients.

To quantify the effects of stimulus strength $|f_{high}-f_{low}|$ on response times t_r, we first used linear regression:

$$t_r=t_0+\frac{m\times|f_{high}-f_{low}|}{100}$$

Regression slope m estimates the change in response time between ambiguous and easiest trials. To fit subjects' chronometric functions on individual sessions, we calculated the re-centred stimulus strength f', such that subjects responded with equal probability to either choice port at $f'=0$, using bias β_0 and slope β_1 estimates from the psychometric fit in (1):

$$f'=f_{high}-f_{low}+\beta_0/\beta_1$$

We then fit subjects' response times t_r to the following function[29]:

$$t_r=\frac{k}{f'}\tanh(\beta_1 f')+t_m$$

Parameter t_m can be thought of as the motor component of the response time, and k sets the magnitude of modulation of response times by the stimulus. We found the values of t_m and k that minimized the mean square error of t_r predictions using MATLAB's *fminsearch* function. We measured the shift of the chronometric function produced by stimulation q, adding it to the response time model:

$$t_r=\frac{k}{f'+qS}\tanh(\beta_1(f'+qS))+t_m$$

To avoid local minima, we re-ran *fminsearch* 100 times using random starting parameter values and selected the set of parameter estimates with the smallest mean square error. Sites for which the fitting procedure failed to converge or produced extreme estimates of the chronometric shift (greater than 200 tones per s) were excluded from further analysis.

In summary plots, linear regression using the ordinary least squares method was used to evaluate the relationship between frequency tuning and stimulation-evoked choice biases. Confidence intervals for regression fits were estimated using bootstrap resampling. A small number of sites (2 out of 59 using non-specific cortical stimulation; 4 out of 56 using striatal axonal stimulation) produced extreme choice biases (greater than 200 tones per s) outside the stimulus range tested in the task and were excluded from regression analysis. Including these sites did not alter the conclusion that striatal axonal stimulation tended to bias subjects in the direction associated with the preferred frequency of the stimilation site ($P=0.03$, signed-rank test).

As we expected that the effects of inactivation would only be detectable when a large fraction of the local population of corticostriatal neurons were silenced, we excluded sites with low Arch expression near the inactivation site (greater than 1,000 cells) in the analysis of behavioural effects of Arch-inactivation in Fig. 3c. For two fibres in one of the rats we could not locate the tracks in histological sections and precisely estimate cell counts. Excluding the behavioural effects of inactivation at these fibres from Fig. 3c did not affect our conclusions ($P=0.014$ for linear regression of choice bias and frequency tuning). Furthermore, the relationship between inactivation choice bias and tuning was unchanged whether we selected sites with greater than 250 neurons ($P=0.012$) or greater than 500 neurons ($P=0.0052$) near the fibre.

Analysis of electrophysiology data. To isolate single units, spikes were manually clustered using MClust (MClust-3.5, http://redishlab.neuroscience.umn.edu/MClust/MClust.html). Neurometric functions were computed using the first 200 ms of the auditory response and only included trials in which the rat remained in the centre port for at least that period of time. We selected neurons whose firing rate during that epoch was greater than or equal to 0.5 Hz. We used leave-one-out cross-validation to determine neurometric thresholds and frequency preference for each neuron. Specifically, for each trial we used ROC (receiver operating characteristic) analysis, including firing rates on all other trials in the recording session, to select a firing rate threshold that best discriminated the frequency content of the auditory stimulus and to determine whether the neuron prefers high or low frequency stimuli. Trials in which the firing rate was greater than or equal to the discrimination threshold were scored as reporting the preferred frequency of the neuron. The neuronal choices were then fit with a logistic regression model (see equation (1)).

To calculate peristimulus time histograms (PSTHs), neuronal firing rates were smoothed with a causal half-Gaussian kernel ($\sigma=5$ ms). Confidence intervals were derived through bootstrap resampling.

For each Arch-expressing corticostriatal neuron that we encountered, we delivered light at different fibres along the array to estimate the maximum distance at which light delivery could reduce the neuron's firing by 50%. We took this distance to be the mean of the distances to the furthest fibre for which inactivation was greater than 50% and the closest fibre for which inactivation was less than 50%. The likelihood of inactivation at a given distance was estimated as the fraction of neurons inactivated at that point.

Histology and cell-count analysis. At the end of the experiment, rats were deeply anaesthetized with ketamine and medetomedine. Small electrolytic lesions were made by passing 30 μA direct cathodal current through each tetrode for approximately 10 s, marking the final position of the tetrode tip. The rats were then perfused with 4% paraformaldehyde (PFA), their brains were extracted and post-fixed in 4% PFA overnight. The brains were cut into 100-μm sections and mounted using Vectashield (Vector Laboratories) for confocal microscopy. To ensure that HSV-mediated labelling was confined to corticostriatal neurons, we verified that viral expression was absent in adjacent brain structures.

To quantify the depth distribution of opsin expression, we measured the distance from each fluorescent cell soma to the pia as a fraction of total cortical thickness. To estimate the number of neurons affected by optogenetic manipulations, confocal stacks 50 μm in depth were acquired from alternate sections. The sections were registered using rigid registration maximizing the cross-correlation of fluorescence images of adjacent sections. The locations of ChR2- or Arch-expressing neurons were identified manually. Fibre tracks were identified with the help of electrolytic lesions and DiI labelling. Using the locations of the ends of the tracks, we estimated that processing resulted in approximately 10% shrinkage of the tissue. We estimated the location of the fibre tip during each inactivation session and counted the number of expressing neurons within 1 mm from the fibre at 35 sites illuminated with 5 mW light. At 6 sites illuminated at 2.5 mW we reduced the radius according to square root of the power to 0.7 mm. Excluding these sites from the analysis did not affect our conclusions ($P=0.036$, linear regression of cell count and choice bias). As we only identified cells within a 50-μm stack every 200 μm, our estimate of the total number of manipulated cells is four times this count.

28. Kelly, J. B. & Masterton, B. Auditory sensitivity of the albino rat. *J. Comp. Physiol. Psychol.* **91,** 930–936 (1977).
29. Palmer, J., Huk, A. & Shadlen, M. The effect of stimulus strength on the speed and accuracy of a perceptual decision. *J. Vis.* **5,** 376–404 (2005).